Archives of Cardiovascular Disease (2016) 109, 87—95

Available online at ScienceDirect www.sciencedirect.com

Elsevier Masson France EM|consulte www.em-consulte.com/en

CLINICAL RESEARCH

3D transthoracic echocardiography to assess pulmonary valve morphology and annulus size in patients with Tetralogy of Fallot

L'échocardiographie 3D transthoracique pour évaluer la morphologie de valve pulmonaire et la taille de l'anneau chez les patients avec tétralogie de Fallot

Khaled Hadeed[a,*], Sébastien Hascoët[a], Romain Amadieu[a], Yves Dulac[a], Sophie Breinig[a], Alexandre Cazavet[b], Fabio Cuttone[b], Bertrand Léobon[b], Philippe Acar[a]

[a] *Pediatric Cardiology Unit, Children's Hospital, Toulouse University Hospital, Toulouse, France*
[b] *Pediatric Cardiac Surgery Unit, Children's Hospital, Toulouse University Hospital, Toulouse, France*

Received 24 September 2015; accepted 8 December 2015
Available online 5 February 2016

KEYWORDS
Pulmonary valve;
Pulmonary annulus;
Three-dimensional echocardiography;
Two-dimensional echocardiography;
Cardiac computed tomography

Summary
Background. — Accurate evaluation of the pulmonary valve (PV) is crucial before surgical repair of Tetralogy of Fallot (TOF).
Aims. — To assess PV and pulmonary annulus (PA) morphology using three-dimensional (3D) transthoracic echocardiography (TTE) in infants referred for surgical repair of TOF. Also, to compare PA measurements obtained by 3D TTE with those from other imaging modalities, including two-dimensional (2D) TTE and computed tomography (CT), with reference to surgical measurements.
Methods. — 3D zoom mode was used to assess PV morphology. 2D TTE and CT PA diameters were compared to both vertical and horizontal diameters obtained from 3D datasets. Surgical PA diameters were measured using Hegar's dilators.

Abbreviations: 2D, two-dimensional; 3D, three-dimensional; 3D max, maximum diameter by 3D TTE; 3D mean, mean diameter by 3D TTE; 3D min, minimum diameter by 3D TTE; CI, confidence interval; CT, computed tomography; ECG, electrocardiogram; MPR, Multiplanar reformatting; PA, pulmonary annulus; PV, pulmonary valve; SD, standard deviation; TOF, Tetralogy of Fallot; TTE, transthoracic echocardiography.

* Corresponding author. Children's Hospital, Pediatric Cardiology, 330, avenue de Grande-Bretagne, TSA 70034, 31059 Toulouse cedex 9, France.
E-mail address: drhadeed@hotmail.fr (K. Hadeed).

http://dx.doi.org/10.1016/j.acvd.2015.12.001

Results. — A total of 29 patients with TOF (median [range] age 6 [3—24] months) were included and all successfully underwent 2D and 3D TTE; 22 also underwent CT. The number of pulmonary leaflets could be visualized in 24 patients (82.8%), with complete concordance with surgical findings. Vertical diameter was significantly longer than horizontal diameter ($P < 0.001$)—underlying PA eccentricity—and was more important in bicuspid than tricuspid valves. Correlations between 2D and 3D TTE diameters were good. Surgical diameter was better correlated with 2D and 3D diameters than with CT diameter. 3D minimum, 2D and CT diameters were significantly lower than surgical diameters, but 3D mean and maximum diameters were not.
Conclusion. — 3D TTE is accurate to assess PV morphology and PA size in patients with TOF. 2D TTE and CT underestimate PA diameter with reference to surgical diameter, however 3D mean and maximum diameters did not differ significantly.

MOTS CLÉS
Valve pulmonaire ;
Anneau pulmonaire ;
Échocardiographie tridimensionnelle ;
Échocardiographie bidimensionnelle ;
Scanner cardiaque

Résumé
Contexte. — L'évaluation de la valve pulmonaire est cruciale avant la correction chirurgicale de la tétralogie de Fallot.
Objectifs. — Évaluer la morphologie de la valve et de l'anneau pulmonaire par l'échocardiographie tridimensionnelle (3D) chez les patients avec Fallot. Comparer les mesures de l'anneau pulmonaire obtenues par 3D avec d'autres modalités d'imagerie (échocardiographie bidimensionnelle [2D] et scanner cardiaque), en référence aux mesures chirurgicales.
Méthodes. — Le 3D zoom a été utilisé pour décrire la morphologie de la valve pulmonaire. Les diamètres en 2D et en scanner ont été comparés aux diamètres vertical et horizontal de l'anneau obtenus à partir des volumes 3D. Le diamètre chirurgical a été mesuré par la bougie de Hegar.
Résultats. — Un total de 29 patients avec Fallot ont été inclus (l'âge médian [intervalle] était de 6 [3—24] mois). Des échocardiographies 2D et 3D ont été effectuées sur tous les patients ; parmi ces derniers, 22 ont eu un scanner cardiaque. Un nombre des feuillets pulmonaires a été visualisé chez 24 patients (82,8 %) avec une complète concordance peropératoire. Le diamètre vertical était plus grand que l'horizontal soulignant l'excentricité de l'anneau pulmonaire, celle-ci était plus importante pour la bicuspidie que pour la valve tricuspide. La corrélation entre le diamètre 2D et 3D était excellente. Le diamètre chirurgical était mieux corrélé avec les diamètres 2D et 3D qu'avec le diamètre scanner. Les diamètres 2D et scanner étaient significativement inférieurs au diamètre chirurgical. Celui-ci n'avait pas de différence significative avec les diamètres moyen et maximal 3D.
Conclusion. — L'échocardiographie 3D est fiable pour évaluer la valve et l'anneau pulmonaire chez les patients avec Fallot. L'échocardiographie des diamètres 2D et le CT sous-estiment le diamètre chirurgical, cependant les diamètres 3D ne diffèrent pas significativement.

Background

Tetralogy of Fallot (TOF) is one of the most common forms of cyanotic congenital heart disease [1]. The objective of the surgical repair is to close the shunt and relieve the right ventricular outflow tract obstruction. The aim is to preserve the pulmonary valve (PV) when possible, to prevent late complications [2,3]. However, transannular patch is sometimes necessary when the PV is severely dysplastic or the size of the pulmonary annulus (PA) is not adequate [4]. Morphological assessment of PV is crucial before surgical repair of TOF. Assessment of PV using conventional two-dimensional (2D) transthoracic echocardiography (TTE) is hard to achieve, as the short-axis view of the valve cannot be obtained. Previous studies have highlighted the interest of three-dimensional (3D) TTE to describe PV and PA in adult populations with or without congenital heart diseases [5,6], but little is known about its use in children. We describe the PV and PA morphology using 3D TTE in children with TOF referred for surgical repair, and compare PA measurements obtained by 3D TTE with other imaging modalities, including 2D TTE and cardiac computed tomography (CT), with reference to surgical measurements as the gold standard.

Methods

Patient characteristics

Consecutive patients referred for surgical repair of TOF were included prospectively. All patients underwent a complete 2D TTE assessment followed by 3D TTE assessment of PV. Some patients also underwent multidetector-row CT within 1 day of echocardiographic assessment. Indications for CT in these patients were to further investigate the pulmonary tree and/or the coronary arteries. Informed consent was obtained from each patient's legal representative. The study protocol was approved by our institutional review board.

Echocardiographic examination

2D TTE was performed using the IE33 ultrasound system (Philips Medical Systems, Andover, MA, USA). After a full echocardiographic evaluation, PA diameter was obtained by 2D TTE from the parasternal short-axis view at the level of the aortic valve. PA diameter was measured at mid-systole between the insertions of the two cusps hinge point using 2D zoom mode as recommended in guidelines [7] (Fig. 1).

3D TTE of the PV was performed at the end of the 2D TTE study for all patients—from the parasternal view—using X7-2 and X5-1 matrix probes (Philips Medical Systems). Live 3D zoom mode was used to allow a more focused visualization of PV. Attention was paid to optimize gain and brightness. Vision H was chosen to ameliorate visualization of valve leaflets, as this vision can provide depth perception (by coding orange for nearer structures and blue for further structures). After acquisition of 3D volume, the image was rotated 90° down to provide an en face view of the PV from the perspective of the right ventricular outflow tract (Fig. 2). 3D datasets were stored digitally and transferred to a dedicated workstation (QLab 9, Philips Medical Systems) for offline analysis.

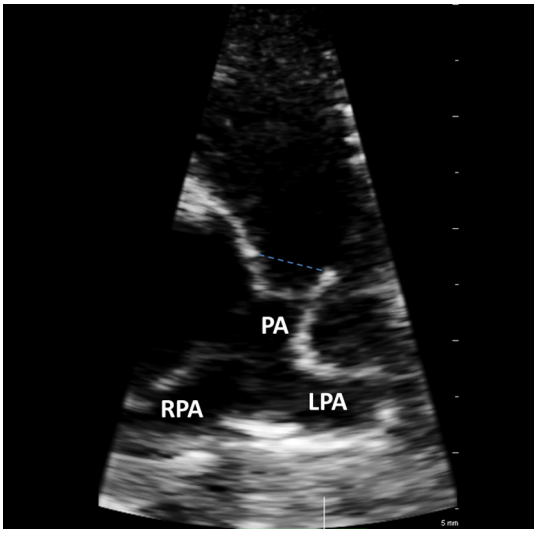

Figure 1. Measurements of PA diameter by 2D TTE using zoom mode. 2D: two-dimensional; LPA: left pulmonary artery; PA: pulmonary annulus; RPA: right pulmonary artery; TTE: transthoracic echocardiography.

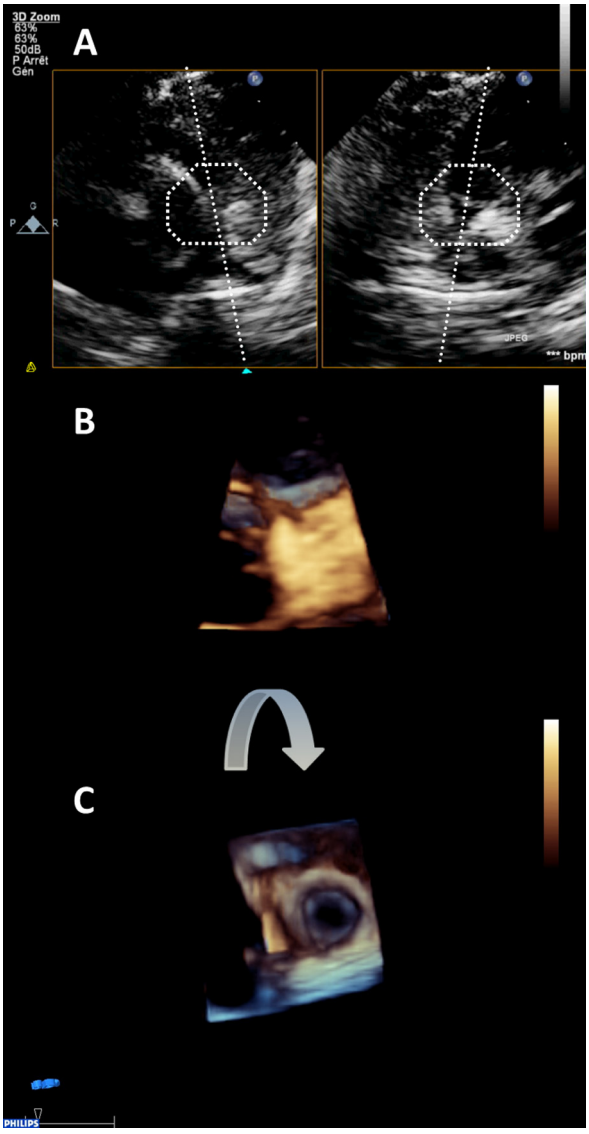

Figure 2. Protocol for 3D zoom mode acquisition. A. From the parasternal short-axis view, a 2D biplane of the PV could be obtained. B. The box of the region of interest was adjusted to include the totality of the PV in the two planes. C. After volume acquisition, it was then rotated 90° down to obtain an en face view of the PV seen from the perspective of the right ventricular outflow tract. 2D: two-dimensional; 3D: three-dimensional; PV: pulmonary valve.

CT examination

Multidetector-row CT was performed using a 64-slice Somatom Definition CT-scanner (Siemens, Forchheim, Germany) without sedation in all patients. Non-electrocardiogram (ECG)-gated CT was obtained using the following protocol: rotation time 330 ms, slice thicknesses 1 mm, tube current 50 mAs and tube voltage 80 kVp. ECG-gated CT was performed in patients with suspected coronary artery anomalies. An iodinated contrast (Xenetix 300; Guerbet, France) was injected into all patients with a power injector. The volume injected was adjusted to the child's weight (2 mL/kg). PA diameter was obtained from axial reconstructed images (maximum-intensity projection)

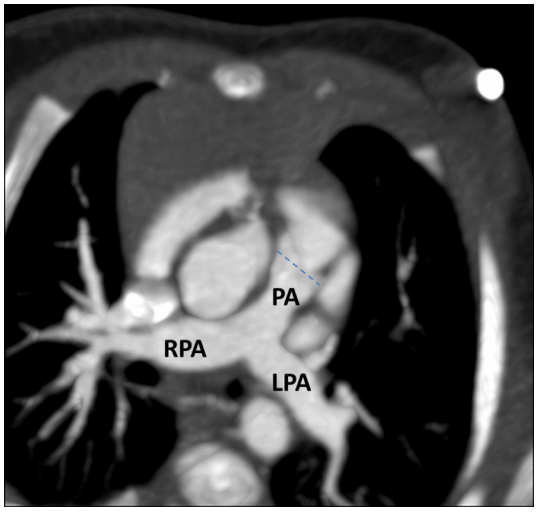

Figure 3. Measurement of the PA by multidetector-row CT from axial view (maximum-intensity projection). CT: computed tomography; LPA: left pulmonary artery; PA: pulmonary annulus; RPA: right pulmonary artery.

at the level of the pulmonary artery, by measuring the distance between the hinge points of the pulmonary cusps following the edge-to-leading edge rule (Fig. 3).

Perioperative PA sizing

After infundibular resection was performed, the PV was inspected by the surgeon and described as bicuspid or tricuspid. Surgical commissurotomy was performed when there was a commissural fusion; the surgical PA diameter was then measured using Higar's dilators (Medline Industries Inc., Mundelein, IL, USA). The surgical PA diameter was considered to be the largest dilator that fitted the pulmonary annulus without forcing. PA diameters are expressed as a Z score calculated from the nomogram of Pettersen et al. [8].

3D TTE dataset analysis

3D TTE image quality was graded according to a simplified four-point scale: poor (PV leaflets not visualized); fair (PV leaflets visualized); good (good visualization of PV leaflets, their coaptation and mobility); and excellent (excellent visualization of PV leaflets, their coaptation, mobility and thickness).

PA sizing from 3D datasets was obtained using Multiplanar reformatting (MPR) mode, with three independent orthogonal cutting planes. Two orthogonal planes were placed in the long axis of the right ventricular outflow tract. The third plane was placed perpendicular to the other two, and moved to the insertion of pulmonary cusps to obtain a short-axis view of the PA (Fig. 4). Both vertical and horizontal diameters of the PA were measured. When the two diameters were different, the largest was called the maximum diameter (3D max) and the smallest was called the minimum diameter (3D min). The 3D mean diameter (3D mean) was calculated as the mean of 3D max and 3D min. PA geometry was expressed by the eccentricity index, which was calculated as $100 \times (3D\ max - 3D\ min)/3D\ max$. An eccentricity index value of zero represents a perfect circle, while a progressively higher eccentricity index represents a more oval geometry.

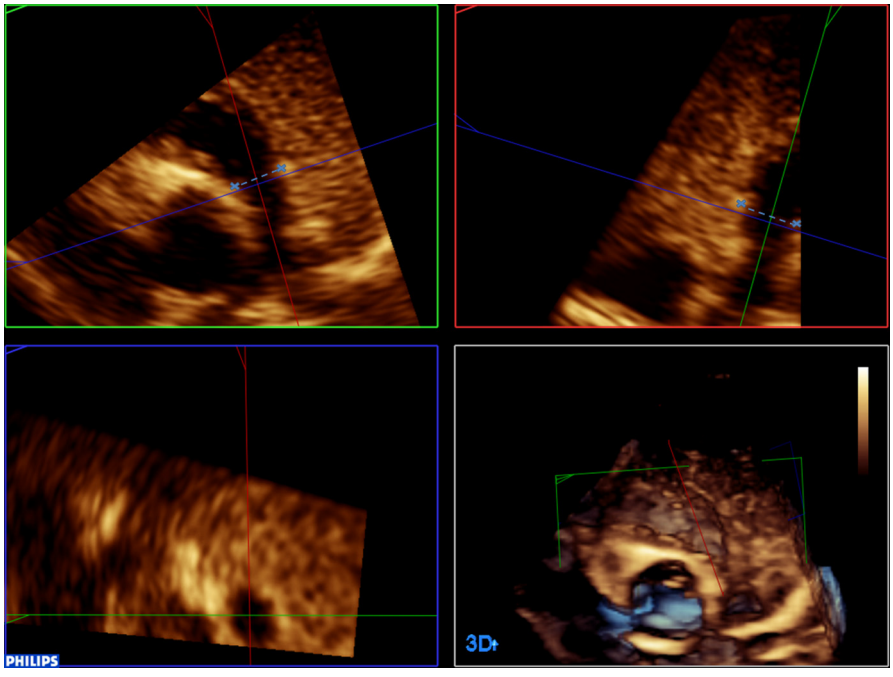

Figure 4. Measurement of the vertical and horizontal diameters of the PA, from a 3D dataset, using MPR mode. The blue plane (bottom left) cuts the 3D volume at the level of PA; the green plane (top left) runs through the PA on its vertical diameter; the red plane (top right) cuts it on its horizontal diameter. 3D: three-dimensional; MPR: multiplanar reformatting; PA: pulmonary annulus.

Statistical analysis

Results are expressed as median (range) for continuous variables or as a number (percentage) for categorical variables. Spearman's correlation coefficients with their 95% confidence intervals (CIs) were used to assess the correlation between PA measurements. The Bland-Altman method was used to further investigate the differences between measurements. Statistical differences were considered significant when the P value was < 0.05. Statistical analyses were performed using Stata® 11.2 software (StataCorp LP, College Station, TX, USA).

Results

Population

Twenty-nine consecutive patients referred for surgical correction of TOF were included prospectively. Their median (range) age was 6 (3—24) months; and weight was 6.5 (4.4—13.5) kg. Six (20.7%) of the patients underwent a palliative intervention for severe cyanosis during the neonatal period (four patients had Blalock-Taussig anastomosis and two had percutaneous pulmonary valvuloplasty).

3D TTE of the pulmonary valve

3D TTE of the PV was feasible in all patients. Image quality was excellent in six patients (20.7%), good in eight (27.6%), fair in 10 (34.5%) and poor in five (17.2%). The number of PV leaflets could be visualized in 24 patients (82.8%). Among these, the PV was bicuspid (Fig. 5A, Video 1A) in 18 patients and tricuspid (Fig. 5B, Video 1B) in six patients. These finding were confirmed perioperatively with complete concordance. In the remaining five patients, the leaflet number could not be determined by 3D TTE, but they were subsequently described by the surgeon as bicuspid in three patients and tricuspid in two patients. Overall, bicuspid PV was significantly more common than tricuspid PV (72.4% vs 27.6%; $P < 0.001$).

In the two patients who underwent pulmonary valvuloplasty in the neonatal period, the PV was bicuspid in both. In one of them, there was a residual fusion of the left commissure, while the right commissure was wide open. In the other patient, there was a flail of the anterior leaflet of the PV with restriction of the posterior leaflet (Fig. 6).

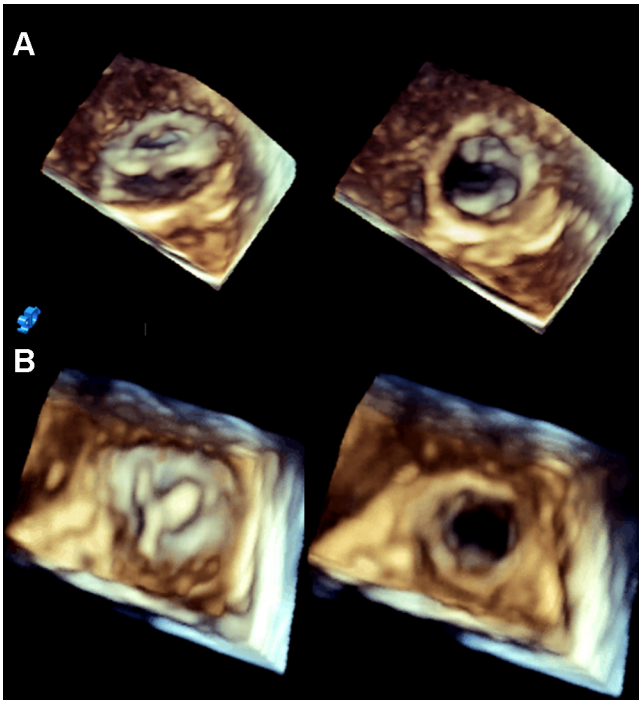

Figure 5. 3D zoom mode demonstrating an en face view from the perspective of the right ventricle of A. a bicuspid and B. a tricuspid PV, at systole (left) and diastole (right). The leaflet number could be seen, as well as their thickness and coaptation. 3D: three-dimensional; PV: pulmonary valve.

3D TTE and pulmonary annulus

The PA could be visualized and assessed using MPR mode in all patients. The median (range) vertical diameter was significantly longer than the horizontal diameter (8.0 [5.7—15.5] vs 6.7 [4.5—14.5]; $P < 0.001$). The mean ± standard deviation (SD) difference between the vertical and horizontal diameters was 1.3 ± 0.8 mm. The median (range) eccentricity index of the PA was 13% (3—31%). The PA was significantly more asymmetric when the PV was bicuspid rather than tricuspid (eccentricity index 14% vs 7%; $P = 0.0002$).

Comparison of PA measurements between imaging modalities

A total of 22 patients (75.9%) underwent multidetector-row CT. PA diameters obtained from the different imaging modalities and perioperative measurements are reported in Table 1. There were good correlations between 2D TTE diameter and 3D min, 3D mean, and 3D max and CT diameters (Table 2). CT diameter had good correlations with 3D min and 3D mean, but less with 3D max). Surgical diameter was

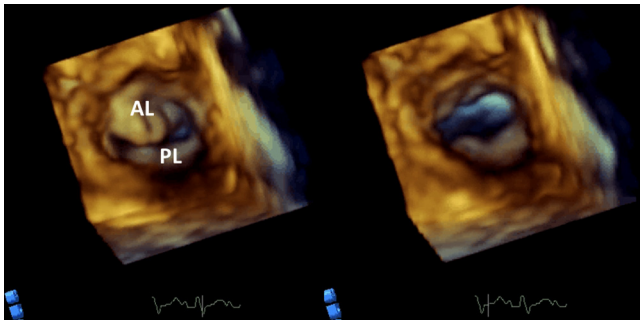

Figure 6. 3D TTE of the PV in a patient who underwent pulmonary angioplasty in the neonatal period at diastole (left) and systole (right). The PV is bicuspid, with flail of the anterior leaflet at diastole, while the posterior leaflet is thickened and sclerotic with low mobility. The zone of malcoaptation between the two leaflets could also be seen at diastole. 3D: three-dimensional; AL: anterior leaflet; PL: posterior leaflet; PV: pulmonary valve; TTE: transthoracic echocardiography.

Table 1 PA diameters obtained by different imaging modalities in our population ($n = 29$).

	Median	95% CI	Minimum	Maximum
2D TTE diameter (mm)	7.0	6.0—8.0	5.0	15.5
3D min (mm)	6.7	6.0—8.5	4.5	14.5
3D max (mm)	8.0	7.0—9.5	5.7	15.5
3D mean (mm)	7.3	6.5—9.0	5.4	15.0
Eccentricity index (%)	13.0	9.0—18.0	3.0	31.0
CT diameter (mm)[a]	7.0	6.4—8.0	5.2	14.8
Surgical diameter (mm)	8.0	6.0—9.0	5.0	15.0

2D: two-dimensional; 3D: three-dimensional; 3D max: maximum diameter by 3D TTE; 3D mean: mean diameter by 3D TTE; 3D min: minimum diameter by 3D TTE; CI: confidence interval; CT: computed tomography; PA: pulmonary annulus; TTE: transthoracic echocardiography.
[a] In 22 patients.

Table 2 Comparison of PA diameters by different imaging modalities ($n = 29$).

	2D TTE diameter	3D min	3D max	3D mean	CT diameter[a]	Surgical diameter
2D TTE diameter	1					
3D min	0.92[b]	1				
3D max	0.90[b]	0.95[b]	1			
3D mean	0.92[b]	0.98[b]	0.99[b]	1		
CT diameter[a]	0.91[b]	0.89[b]	0.82[b]	0.87[b]	1	
Surgical diameter	0.78[b]	0.76[b]	0.79[b]	0.78[b]	0.61[c]	1

Data are Spearman's correlation coefficients (r). 2D: two-dimensional; 3D: three-dimensional; 3D max: maximum diameter by 3D TTE; 3D mean: mean diameter by 3D TTE; 3D min: minimum diameter by 3D TTE; CT: computed tomography; PA: pulmonary annulus; TTE: transthoracic echocardiography.
[a] In 22 patients.
[b] $P < 0.0001$.
[c] $P = 0.06$.

better correlated with 2D TTE and all 3D TTE diameters but less with CT diameter (Table 2).

2D TTE and CT diameters did not differ significantly from 3D min diameter ($P = 0.12$). However, they were significantly lower than 3D mean and 3D max diameters ($P < 0.001$). When compared with perioperative sizing, 2D TTE, CT and 3D min diameters were significantly lower than surgical diameters ($P < 0.05$, $P = 0.04$ and $P < 0.01$, respectively; Fig. 7). However, 3D mean and 3D max diameters did not differ significantly from surgical diameters ($P = 0.32$ and $P = 0.08$, respectively; Fig. 7).

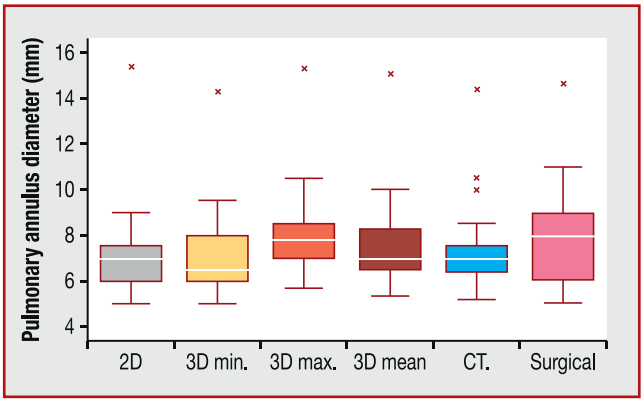

Figure 7. Box plot comparing measurements of PA diameter obtained by different imaging modalities with the surgical diameter. Boxes show first and third quartiles; horizontal lines show medians; whiskers show interquartile range; outliers are shown as crosses. 2D: two-dimensional TTE diameter; 3D: three-dimensional; 3D max: maximum diameter by 3D TTE; 3D mean: mean diameter by 3D TTE; 3D min: minimum diameter by 3D TTE; CT: computed tomography; PA: pulmonary annulus; TTE: transthoracic echocardiography.

Bland-Altman analysis revealed a good agreement between 3D mean and 3D max diameters with surgical diameters (mean differences of -0.3 ± 1.15 mm and 0.3 ± 1.15 mm, respectively; Fig. 8). This difference was more important when the PA diameter was smaller. Bland-Altman agreements for 2D, 3D min and CT diameters with surgical diameters were lower, as illustrated in Fig. 8.

A surgical diameter Z score of -2 was the threshold used by the surgeon to preserve the PA. The 3D mean diameter was the most predictive of conserving PA: a value of Z score at -1.6 had a sensitivity of 76.5% and a specificity of 91.7% to predict surgical conservation of the PA (Fig. 9).

Impact of PV morphology on surgical results

The surgical diameter Z score tended to be lower when the PV was bicuspid rather than tricuspid (median -1.4 vs -0.5), although the difference was not statically significant ($P = 0.19$; Table 3). In this series, the PA was preserved in

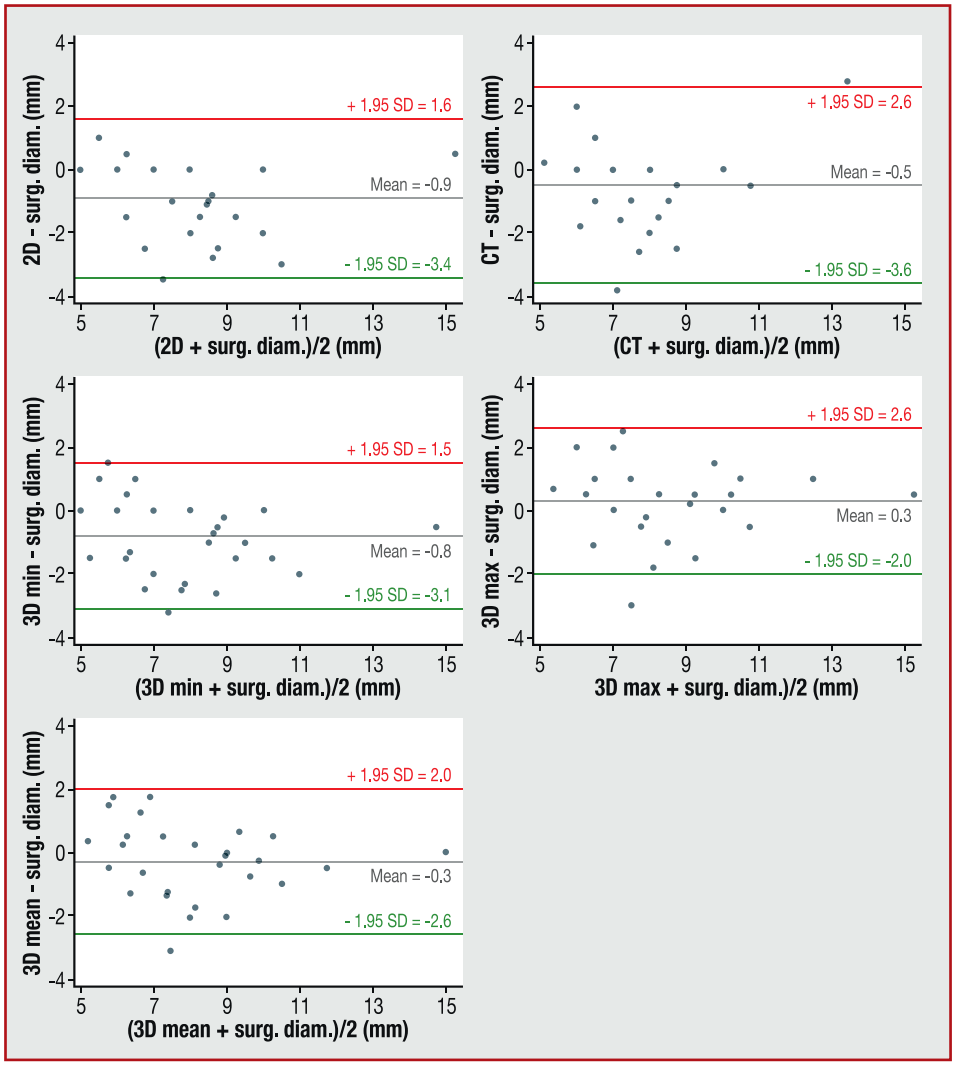

Figure 8. Bland-Altman analysis displaying the differences between PA diameters obtained by the different imaging modalities compared with the surgical diameter. 2D: two-dimensional TTE diameter; 3D: three-dimensional; 3D max: maximum diameter by 3D TTE; 3D mean: mean diameter by 3D TTE; 3D min: minimum diameter by 3D TTE; CT: computed tomography diameter; PA: pulmonary annulus; SD: standard deviation; surg. diam.: surgical diameter; TTE: transthoracic echocardiography.

all patients with a surgical diameter Z score more than −2, which represented 16 patients (55.2%). This included 5/8 tricuspid valves (62.5%) and 11/21 bicuspid valves (52.4%) ($P = 0.41$). No significant residual pulmonary stenosis was observed immediately or after 20-month follow-up, except one patient required a percutaneous pulmonary valvuloplasty 1 year after surgery.

Discussion

Assessment of PV morphology using 2D TTE is challenging. 2D TTE cuts the PV in its long axis, so only two cusps can be visualized simultaneously. A short-axis view of the PV is not generally obtained by 2D TTE, although in rare cases of patients in whom the orientation of the pulmonary artery

Table 3 Comparison between bicuspid and tricuspid PVs.

	Total population ($n = 29$)	Bicuspid PV ($n = 21$)	Tricuspid PV ($n = 8$)	P
Surgical diameter Z score	−1.2 (−3.6 to −0.4)	−1.4 (−3.7 to −0.6)	−0.5 (−2.5 to 0)	0.19
Eccentricity index (%)	13.0 (9–18)	14.0 (13–19)	7.0 (6–7)	0.0002
Valve conserved	16 (55.2)	11 (52.4)	5 (62.5)	0.41

Data are expressed as median (95% confidence interval) or number (%). PV: pulmonary valve.

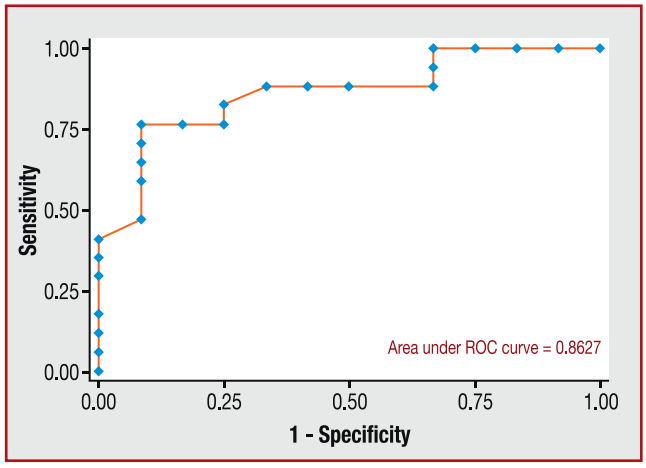

Figure 9. ROC curve of 3D mean Z score to predict a −2 surgical diameter Z score threshold. 3D: three-dimensional; ROC: receiver operating characteristic.

is unusual, this could be possible [9]. The advantage of 3D TTE is that it provides volumetric datasets that can then be cropped and reoriented to assess the zone of interest from any perspective. Our study demonstrates the accuracy of 3D TTE to assess PV in patients with TOF. In this study, an en face view of the PV could be obtained in all patients. The image quality was sufficient in the majority of our patients (82.8%) to assess PV morphology. The majority of bicuspid PVs could be distinguished by 3D TTE before surgery. We used 3D zoom mode for the acquisition of 3D images. As an advantage, as opposed to other 3D acquisitions, this mode eliminates the need for cropping the volume as the volume is defined manually before fitting the zone of interest. Furthermore, this mode permits a more focused image of the target structure, provides artefact-free images with adequate image quality, and eliminates other surrounding structures that could prevent good visibility of the PV.

The PV is the valve least studied by 3D TTE among the four cardiac valves, and few data exist in the literature. Kelly et al. [5] demonstrated the feasibility of using 3D TTE in the morphological assessment of PVs in adults without congenital heart disease. In their study, the detection rate of the PV morphology was higher using live 3D zoom mode rather than 3D full volume mode (60% vs 22%). They also demonstrated that 3D image quality was dependent on the initial 2D image quality. This could explain the higher detection rate in our study, as transthoracic acoustic windows are generally better in children than adults. Anwar et al. [6] demonstrated the incremental value of 3D TTE for the assessment of PV in 50 adults with different congenital heart diseases including one patient with TOF. They found that PV morphology could be assessed in 70% of patients and was bicuspid in three patients. However there are no data available concerning this issue in children. Our study is the first to demonstrate the added value of 3D TTE in the description of PV morphology in children with TOF.

Furthermore, our study could provide new information about the geometry of the PA. The vertical diameter of the PA was longer than the horizontal diameter, and the difference between the two diameters was statically significant. This indicates that the PA is not perfectly round, but rather slightly oval, in patient with TOF. This observation does not seem to concern only patients with TOF. Berdajs et al. [10] described the asymmetrical geometry of the pulmonary root in normal hearts by morphometric measurement of the distance between commissures and between the intervalvular triangles. Anwar et al. [6] assessed PV morphology using 3D TTE in adults with different congenital heart diseases. They found that the shape of the PA appeared visually as oval rather than completely circular. The present study extends these results by quantification of this asymmetry using the eccentricity index. Furthermore, we found that the severity of PA asymmetry was different according to the valve morphology, as it was more important in bicuspid than tricuspid valves. No data are available in the literature about this concern. However, these observations seem to be similar to those previously described for the aortic valve [11—13]. Moreover, a recent study found that the aortic annulus, assessed by 3D TTE, was more asymmetric in children with bicuspid aortic valve than in those with tricuspid aortic valve [14]. These similar modifications of aortic annulus and PA geometry in cases of bicuspid and tricuspid valves suggest a common pathophysiology in both situations and need more investigation.

Our study is the first to our knowledge to compare the accuracy of three imaging techniques (2D TTE, CT and 3D TTE) for PA sizing, with reference to surgical sizing as the gold standard. Our results demonstrate that 2D TTE and CT measurements underestimate the surgical diameter, while 3D mean and 3D max diameters have the best agreement with the surgical gold standard sizing, with the mean differences between the two methods being -0.3 ± 1.15 mm and 0.3 ± 1.15 mm, respectively. These relatively wide limits of agreement could be explained by the perioperative sizing, which was done by Hegar's dilators with graduations in 1-mm increments, so a difference inferior to 1 mm could not be appreciated.

One previous study has demonstrated that measurement of the PA from a short-axis view by 2D TTE leads to underestimation of the PA diameter compared to 3D TTE in adult patients [6]. In our study, we can explain this by the asymmetry of the PA—the vertical diameter was significantly longer than the horizontal diameter. 2D TTE measures the distance from the basal attachment of one leaflet to the basal attachment of an adjacent leaflet, and these lines do not necessarily span the maximum diameter of the PA, but provide a tangential profile of the outlet. Hayabuchi et al. [15] found that, although there was an excellent correlation between multidetector-row CT and invasive angiography for the quantification of pulmonary artery sizes in children with congenital heart diseases, the correlation for PA sizing was only moderate. This could be explained by motion artefacts during the cardiac cycle that affect the PV more than the pulmonary arteries.

Preservation of the PV in patients with TOF could prevent the deleterious effects of pulmonary regurgitation, including early and late right ventricular failure and arrhythmia [16,17]. However, to date, there is no agreement about which patients could benefit from conserving surgery compared to the size of the PA [18—20]. In our series, PV was conserved in all patients with surgical diameter Z score more than −2 (55.2%) without significant residual pulmonary stenosis immediately and after 20-month follow-up. 3D

mean diameter was the most predictive of surgical conserving of PA with a good sensitivity and specificity. Although our study design does not address this issue, this demonstrates that PV preservation could be possible even when the PA is hypoplasic. Moreover, the PA tended to be smaller when the PV was bicuspid rather than tricuspid. Although the difference did not reach statistical significance, the preservation of PV was more frequent in tricuspid than bicuspid valves. These results are with agreement with a previous study where they found that a tricuspid PV is a significant marker for success of PV-sparing approach to the repair of TOF [17]. Our study demonstrates that 3D TTE is an interesting non-invasive imaging technique that could enhance understanding of PV morphology and provide accurate measurements of the PA necessary for patient management. Other applications of 3D TTE could be the assessment of PV before percutaneous valvuloplasty of pulmonary stenosis and sizing of the right ventricular outflow tract before implantation of a Melody valve.

Conclusions

3D TTE is an accurate method to describe PV morphology and for PA sizing in infants with TOF. 2D TTE and multidetector-row CT underestimate PA diameter with reference to surgical diameter, however 3D TTE diameters did not differ significantly.

Sources of funding

None.

Disclosure of interest

The authors declare that they have no competing interest.

Appendix A. Supplementary data

Supplementary data associated with this article can be found, in the online version, at http://dx.doi.org/10.1016/j.acvd.2015.12.001.

References

[1] Reller MD, Strickland MJ, Riehle-Colarusso T, Mahle WT, Correa A. Prevalence of congenital heart defects in metropolitan Atlanta, 1998-2005. J Pediatr 2008;153:807—13.
[2] Vida VL, Guariento A, Castaldi B, et al. Evolving strategies for preserving the pulmonary valve during early repair of Tetralogy of Fallot: mid-term results. J Thorac Cardiovasc Surg 2014;147:687—94 [discussion 94-6].
[3] Vida VL, Angelini A, Guariento A, et al. Preserving the pulmonary valve during early repair of Tetralogy of Fallot: anatomic substrates and surgical strategies. J Thorac Cardiovasc Surg 2015;149:1358—63, e1.
[4] Awori MN, Leong W, Artrip JH, O'Donnell C. Tetralogy of Fallot repair: optimal Z-score use for transannular patch insertion. Eur J Cardiothorac Surg 2013;43:483—6.
[5] Kelly NF, Platts DG, Burstow DJ. Feasibility of pulmonary valve imaging using three-dimensional transthoracic echocardiography. J Am Soc Echocardiogr 2010;23:1076—80.
[6] Anwar AM, Soliman O, van den Bosch AE, et al. Assessment of pulmonary valve and right ventricular outflow tract with real-time three-dimensional echocardiography. Int J Cardiovasc Imaging 2007;23:167—75.
[7] Lopez L, Colan SD, Frommelt PC, et al. Recommendations for quantification methods during the performance of a pediatric echocardiogram: a report from the Pediatric Measurements Writing Group of the American Society of Echocardiography Pediatric and Congenital Heart Disease Council. J Am Soc Echocardiogr 2010;23:465—95 [quiz 576-7].
[8] Pettersen MD, Du W, Skeens ME, Humes RA. Regression equations for calculation of Z scores of cardiac structures in a large cohort of healthy infants, children, and adolescents: an echocardiographic study. J Am Soc Echocardiogr 2008;21:922—34.
[9] McAleer E, Kort S, Rosenzweig BP, et al. Unusual echocardiographic views of bicuspid and tricuspid pulmonic valves. J Am Soc Echocardiogr 2001;14:1036—8.
[10] Berdajs D, Lajos P, Zund G, Turina M. Geometrical model of the pulmonary root. J Heart Valve Dis 2005;14:257—60.
[11] Park JS, Choi YW, Shin JS, et al. Validation of three-dimensional echocardiography for quantification of aortic root geometry: comparison with multi-detector computed tomography. J Cardiovasc Ultrasound 2011;19:128—33.
[12] Doddamani S, Bello R, Friedman MA, et al. Demonstration of left ventricular outflow tract eccentricity by real time 3D echocardiography: implications for the determination of aortic valve area. Echocardiography 2007;24:860—6.
[13] Martin R, Hascoet S, Dulac Y, et al. Comparison of two- and three-dimensional transthoracic echocardiography for measurement of aortic annulus diameter in children. Arch Cardiovasc Dis 2013;106:492—500.
[14] Chamberland CR, Sugeng L, Abraham S, Li F, Weismann CG. Three-dimensional evaluation of aortic valve annular shape in children with bicuspid aortic valves and/or aortic coarctation compared with controls. Am J Cardiol 2015;116:1411—7.
[15] Hayabuchi Y, Mori K, Kitagawa T, Inoue M, Kagami S. Accurate quantification of pulmonary artery diameter in patients with cyanotic congenital heart disease using multidetector-row computed tomography. Am Heart J 2007;154:783—8.
[16] Karamlou T, McCrindle BW, Williams WG. Surgery insight: late complications following repair of Tetralogy of Fallot and related surgical strategies for management. Nat Clin Pract Cardiovasc Med 2006;3:611—22.
[17] Parry AJ, McElhinney DB, Kung GC, Reddy VM, Brook MM, Hanley FL. Elective primary repair of acyanotic Tetralogy of Fallot in early infancy: overall outcome and impact on the pulmonary valve. J Am Coll Cardiol 2000;36:2279—83.
[18] Rao V, Kadletz M, Hornberger LK, Freedom RM, Black MD. Preservation of the pulmonary valve complex in Tetralogy of Fallot: how small is too small? Ann Thorac Surg 2000;69:176—9 [discussion 9-80].
[19] Boni L, Garcia E, Galletti L, et al. Current strategies in Tetralogy of Fallot repair: pulmonary valve sparing and evolution of right ventricle/left ventricle pressures ratio. Eur J Cardiothorac Surg 2009;35:885—9 [discussion 9-90].
[20] Stewart RD, Backer CL, Young L, Mavroudis C. Tetralogy of Fallot: results of a pulmonary valve-sparing strategy. Ann Thorac Surg 2005;80:1431—8 [discussion 8-9].